Published in final edited form as:
Biochemistry. 2012 April 3; 51(13): 2867–2878. doi:10.1021/bi201721r.

HIV-1 gp41 Transmembrane Domain Interacts with the Fusion Peptide: Implication in Lipid Mixing and Inhibition of Virus-Cell Fusion

Eliran Moshe Reuven[a], **Yakir Dadon**[a], **Mathias Viard**[b,c], **Nurit Manukovsky**[a], **Robert Blumenthal**[b], and **Yechiel Shai**[a,*]

[a]Department of Biological Chemistry, The Weizmann Institute of Science, Rehovot, 76100 Israel

[b]Basic Research Program, SAIC-Frederick, Inc., NCI-Frederick, Frederick, Maryland 21702

[c]Nanobiology Program, Center of Cancer Research, National Cancer Institute, Frederick, Maryland, USA

Abstract

Fusion of the human immunodeficiency virus (HIV) with target cells is mediated by the gp41 subunit of the envelope protein. Mutation and deletion studies within the transmembrane domain (TMD) of intact gp41 influenced its fusion activity. In addition, current models suggest that the TMD is in proximity with the fusion peptide (FP) at the late fusion stages, but there are no direct experimental data to support this hypothesis. Here we investigated the TMD focusing on two regions: the N-terminal containing the GxxxG motif, and the C-terminal containing the GLRI motif, which is conserved among the TMDs of HIV and the T-cell receptor. Studies utilizing the ToxR expression system combined with synthetic peptides and their fluorescent analogs derived from TMD, revealed that the GxxxG motif is important for TMD self-association, whereas the C-terminal region for its hetero-association with FP. Functionally, all three TMD peptides induced lipid mixing that was enhanced significantly upon mixing with FP. Furthermore, the TMD peptides inhibited virus-cell fusion apparently through their interaction with their endogenous counterparts. Notably, the R2E mutant (in the GLRI) was significantly less potent than the two others. Overall, our findings provide experimental evidence that HIV-1 TMD contributes to membrane assembly and function of the HIV-1 Envelope. Owing to similarities between functional domains within viruses, these findings suggest that the TMDs and FPs may contribute similarly in other viruses as well.

Keywords

lipid mixing; HIV-1 envelope; FRET; synthetic peptides; virus-cell fusion

The infection of a cell by HIV is a well-coordinated event. This process is performed by the envelope glycoprotein (Env- gp160), a type-I integral membrane protein, which is expressed on the surface of the virus and functions as a trimer (1–4). Gp160 is composed of non-

*The Harold S. and Harriet B. Brady Professorial Chair in Cancer Research. To whom correspondence should be addressed. Phone: 972-8934-2711 Fax: 972-8934-4114, Yechiel.Shai@weizmann.ac.il.

Supporting Information

Figure S1: The emission spectra of NBD and Rho labeled peptides.
Figure S2: FRET efficiency between the TMD peptides.
Figure S3: Titration curves of TMD peptides
This material is available free of charge via the Internet at http://pubs.acs.org

covalently attached gp120 and gp41 subunits. Gp120 recognizes CD4 and other co-receptors that together initiate an activated state leading to conformational changes. These result in the exposure of gp41, the key component responsible for the virus-cell fusion process (1, 5–7), schematically presented in Figure 1. The ectodomain of gp41 is composed of an N-terminal fusion peptide (FP), a fusion peptide proximal region (FPPR), N- and C-terminal heptad repeats (NHR and CHR, respectively) that are separated by a loop, a membrane proximal region (MPER), and the transmembrane domain (TMD) (3, 5, 8, 9).

The current knowledge regarding the various states of gp41 during the fusion process has been obtained mainly by high-resolution structures, as well as studies using peptide inhibitors and conformation-specific antibodies (2, 10–13). Accumulating data suggest that there are at least three main gp41 conformations during the fusion process: the first is the native non-fusogenic state, the second is the pre-hairpin conformation (PHI) or pre-fusion step, and the third is the post fusion step (hairpin conformation) also termed the six-helix bundle (SHB) (5, 13–19). Although the participation of FP during the PHI and SHB states has been widely studied, only a few studies focused on the involvement of the TMD in the fusion process. Furthermore, recent studies have suggested that FP and TMD are in proximity during viral fusion (20–22). These studies showed that the monoclonal antibody 2F5 binds ideally to its epitope, the MPER, upon its interaction with the sequence downstream of the FP, the FPRR (21). In addition, both FP and TMD bind the T-cell receptor (TCR) transmembrane complex leading to inactivation of T cells (23, 24). All together these suggest a possible interaction between FP and TMD.

Transmembrane domains (TMDs) of many membrane proteins have been shown to contribute to the assembly of the parental proteins. These interactions are mediated by various motifs (25–31). Among them, the GxxxG motif is the most studied one (27, 32), and it is also located in the gp41 TMD (13, 33, 34). Mutational studies within the TMD in the intact gp41, as well as its complete replacement, revealed that the GxxxG motif contributes to the fusion process (35–37). However, the direct participation of the TMD in the membrane fusion process and its interaction with FP have not been reported. HIV-1 TMD contains, in addition, the GLRI motif, which plays an important role in viral-induced T-cell immuno-modulation (24). However, the role of these motifs during virus-cell fusion is not yet clear. Furthermore, a recent study showed that mutating the Arg residue within the intact protein did not affect the expression or location of Env, but rather, affected its fusion activity (38).

Synthetic peptides corresponding to regions within gp41 serve as a powerful tool to explore the dynamic mechanism underlying gp41-induced membrane fusion (14, 15, 18, 39, 40). As a general trend, mutations within the entire envelope protein that reduced its fusogenic activity also reduced the ability of the corresponding synthetic peptides to induce lipid mixing of model membranes (41).

In this study we characterized the TMD for its ability to homo-assemble within the membrane milieu and to hetero-assemble with FP via distinct regions. We also determined its ability to induce lipid mixing alone, and in combination with FP. Finally, we studied the ability of the peptides to interfere with the native virus-cell fusion process. Besides advancing our understanding of the mechanism underlying virus-cell fusion, this study strengthens FP as a potential entry inhibitor (9, 42) and suggests TMD as a new one too. Previous studies have shown that the TMD and FP in Influenza virus functionally associate during the entry steps (43). Owing to structural and functional similarities between enveloped viruses including subunit composition, the presence of heptad repeats, and the function of the different subunits (FP, TMD and cytoplasmatic tail), our findings suggest that the TMDs and FPs of other viruses may contribute in a similar manner as well.

EXPERIMENTAL PROCEDURES

Construction of the ToxR chimeras

A NheI-BamHI TM-DNA cassette encoding 16 residues of the gp41 WT transmembrane domain (^{686}I V G G L V G L R I V F A V L S^{701}) was inserted between the ToxR transcription activator and the *E. coli* maltose binding protein (MalE) within the ToxR-MalE plasmid. The R2E and GGG constructs contained the WT sequence, with Arg at position 694 mutated to a glutamic acid and the LVG sequence changed to GLV at position 691–693, respectively (Table 1). The sequence of all the constructs was confirmed by DNA sequencing.

Peptide synthesis and purification

Peptides were synthesized by the F-moc solid-phase method on a Rink amide MBHA resin. A lipophilic acid was attached to the N terminus of a resin-bound peptide using standard F-moc chemistry. Briefly, after removal of the F-moc group from the N terminus of the peptide with a solution of 20% piperidine in dimethylformamide (DMF), the fatty acid (10 eq, 1 M in DMF) was coupled to the resin under similar conditions used for the coupling of an amino acid. The peptides were cleaved from the resin by trifluoroacetic acid (TFA) and were purified by RP-HPLC on a C2 reverse phase Bio-Rad semi-preparative column (250×10 mm, 300-Å pore size, 5-μm particle size). The purified peptides were shown to be homogeneous (>95%) by analytical HPLC. The peptides' compositions were confirmed by electrospray mass-spectrometry. A single lysine residue was added to the C-termini of the peptides to confer water solubility to the hydrophobic TM domains. It was previously shown that hydrophobic peptides conjugated to lysine tags were correctly oligomerized and inserted into the membrane (44–46).

In Vivo Detection of homo- and hetero-association of TMDs within the membrane

The ToxR transcription activator can be used successfully to assess weak protein-protein interactions within the *E. coli* membrane. A DNA cassette encoding the gp41 TMD was grafted between the ToxR transcription activator and the maltose binding protein in the ToxR-MalE plasmid (named ToxR-TM-MalE). The plasmid was then transformed into *E. coli* FHK12 cells that contain β-galactosidase, under the control of a *ctx* promoter. Association of the TMDs, in this system, results in association and activation of the ToxR transcription activator, which then becomes active and can bind the *ctx* promoter (47). The amount of homo-association was quantified by measuring the activity of the β-galactosidase reporter gene and by normalizing it to the cell content (OD_{590}) (Miller units). The β-galactosidase activity levels expressed by the GpA TMD sequence were referred to as 100% association. The transformed cells were grown in the presence of chloramphenicol for 18 hr at 37 °C. β-galactosidase activities were quantified in crude cell lysates after adding *o*-nitrophenylgalactosidase and monitoring the reaction at 405 nm for 20 min, at intervals of 30 sec at 28 °C with a Molecular Devices kinetic reader (47, 48). Specific β-galactosidase activities were computed from the V_{max} of the reaction. In order to calculate the percentage of association of each construct, we measured the β-galactosidase activity levels and divided them by the activity of GpA.

Hetero-association was detected using ToxR-TM-MalE -expressing bacteria (WT sequence) grown in the absence or presence of exogenous peptides. Inhibition was calculated as follows:

$$I = 1 - \frac{A_{peptide} - A_{baseline}}{A_{\max} - A_{baseline}}, \quad (1)$$

where I represents the inhibitory ability of the peptide, $A_{peptide}$ is the activity of ToxR-TM-MalE in the presence of a peptide, A_{max} is the maximal activity of ToxR-TM- MalE without the peptide, and $A_{baseline}$ is the baseline activity of the monomer A_{15} plasmid (47).

Expression levels of ToxR-TM-MalE chimeric protein

We performed Western blot analysis in order to determine whether changes in the sequence of the TM domain affected the expression levels of the chimera proteins. Specifically, aliquots of 10 μl FHK12 cells, each with a different plasmid or in the presence of a different peptide, were mixed with a sample buffer, boiled for 5 min, subjected to 12% SDS-PAGE, and then transferred to nitrocellulose. The primary antibody used was anti-Maltose binding protein. The “Phototope-HRP Western Blot Detection System” from Cell Signaling Technology was used for detection. The presence of MBP in the periplasm was confirmed by growth on minimal maltose media.

Fluorescent labeling of the peptides

The F-moc protecting group was removed from the N-terminus of the resin-bound peptides by incubation with piperidine for 12 minutes, whereas all the other reactive amine groups of the attached peptides were kept protected. The resin-bound peptides were washed twice with dimethylformamide (DMF), and then treated with Rhodamine (Rho), in anhydrous DMF containing 2% N,N-diisopropylethylamine (DIEA), leading to the formation of a resin-bound N-Rho-peptide. After 24 hr, the resin was washed thoroughly with DMF and then with methylene chloride (DCM). The labeled peptides were cleaved from the resin and purified as described previously. The same procedure was performed to label the peptides with 4-fluoro-5-nitrobenzoxadiazole (NBD).

Preparation of Large unilamellar vesicles (LUV)

Thin films of PC (L-α-phosphatidylcholine, dipalmitoyl (C16:0), Sigma chemical STL, MO, USA) and Cholesterol (Sigma chemical STL, MO, USA) mixed at a molar ratio of 9:1, respectively, were generated by dissolving the lipids in a 2:1 (v/v) mixture of $CHCL_3$/MeOH, and then dried under a stream of nitrogen gas while they were rotated. Two populations of films were generated: (1) a PC:Chol mixture as described above, termed “unlabeled” and (2) the same lipid mixture containing a 0.6% molar of NBD-PC and Rho-PC each, termed “labeled”. The films were sealed with argon gas to prevent oxidation of the lipids and then stored at −20° C. Before the experiment, the films were suspended in PBS buffer and vortexed for 1 min. The lipid suspension underwent five cycles of freezing-thawing followed by extrusion through polycarbonate membranes with 1-μm and 0.1-μm diameter pores for 21 times to create large unilamellar vesicles.

Membrane binding assay

The fluorescence of NBD is sensitive to its environment (49, 50). The fluorescence quantum yield is low in solutions and high in the membrane-bound state. This allows monitoring the binding of NBD-labeled peptides to membranes. The degree of peptide association with PC:Cholesterol LUVs dissolved in PBS, was measured by adding increasing amounts of vesicles to 0.2 μM NBD-labeled peptides (400 μL PBS and 1% dimethylsulfoxide (DMSO)) under constant mixing. The fluorescence intensity was measured as a function of the lipid:peptide molar ratio, with excitation set at 465 nm (10-nm slit) and emission set at 530 nm (10-nm slit). The system reached binding equilibrium (Fmax) at a certain lipid/peptide ratio, and therefore the affinity constant could be calculated from the relationship between the equilibrium level of NBD-labeled peptide emission and the lipid concentration, using a steady-state affinity model. The affinity constants were thus determined by nonlinear least-squares (NLLSQ) analysis. The NLLSQ fitting was done using the following equation:

$$Y(x)=K_a*X*F_{max}/(1+K_a*X) \quad (2)$$

where X is the lipid concentration, Fmax is the maximal difference in the emission of NBD-labeled peptide before and after the addition of the lipids (it represents the maximum lipid peptide bound or the equilibrium-binding response), and Ka is the affinity constant, in M^{-1}. Kd was extrapolated from the Ka values according to the equation:

$$K_d=1/K_a \quad (3)$$

Measurements of fluorescence energy transfer (FRET)

The FRET experiments were performed by using NBD and Rho labeled peptides as fluorescence donor and acceptor, respectively. The wavelength of the maximal emission of NBD is at 525–530nm (when it is in a hydrophobic environment). This wavelength overlaps with the excitation wavelength of Rho. Therefore, when NBD and Rho are in close proximity, excitation of NBD at 467 nm results in a decrease in the maximal emission of NBD at ~528 nm, and an increase in the maximal emission of Rho at ~580 nm. Fluorescence spectra were obtained at room temperature, with excitation set at 467 nm (10-nm slit) and emission scan at 500–600 nm (10-nm slit). In a typical experiment, a NBD-labeled peptide (stock solution in DMSO) was first added to a dispersion of 400 μL solution of PC LUV dissolved in PBS (100 μM, final peptide concentration 0.4 μM, and a maximum of 0.25% (v/v) DMSO). This was followed by the addition of a Rho labeled peptide in several sequential doses ranging from 0.0125 μM to 0.2 μM (stock solution in DMSO). Fluorescence spectra were obtained before and after addition of the Rho labeled peptide. The efficiency of energy transfer (E) was determined by measuring the decrease in the quantum yield of the donor, as a result of the energy transfer to the acceptor. E was determined experimentally from the ratio of the fluorescence intensities of the donor in the presence (I_{da}) and the absence (I_d) of the acceptor, at the wavelength of the donor's maximal emission (530nm). The percentage of transfer efficiency (E) is given by:

$$E(\%)=(1-I_{da}/I_d)\times 100 \quad (4)$$

Subtracting the signal produced by the acceptor-labeled analogue alone corrected the contribution of the emission of the acceptor as a result of direct excitation. The contribution of buffer and vesicles was subtracted from all measurements.

Peptide-induced lipid mixing

All fluorescence measurements were performed on a Cary-Eclipse fluorescence spectrophotometer (Agilent technologies, Santa Clara, CA, USA) at 25°C. The extent of lipid mixing of LUV induced by a peptide was measured using a fluorescence-probe dilution assay (51). In this assay, vesicles labeled with a combination of fluorescence energy transfer donor (NBD) and acceptor (rhodamine) lipid probes, respectively, are mixed with unlabeled vesicles. FRET is detected as increased rhodamine emission at 585 nm and decreased NBD emission at 530 nm as a result from NBD excitation at 470 nm. This is because the average spatial separation of the probes is increased upon fusion of labeled membranes with unlabeled membranes. To measure the capacity of the peptides to induce Lipid mixing, PC:Chol LUVs containing 0.6 molar % each of NBD-PE and Rho-PE, were prepared in PBS as described above. A 1:9 mixture of labeled and unlabeled vesicles (100 μM total phospholipid concentration) was suspended in 400 μl of PBS, and a small volume of a peptide in stock solution of DMSO was added. The increase in NBD fluorescence at 530 nm (10-nm slit) was monitored, with the excitation set at 467 nm (10-nm slit). The fluorescence intensity before the addition of the peptide was referred to as 0% lipid mixing, and the

fluorescence intensity upon addition of reduced Triton X-100 (0.05% (v/v)) was referred to as 100% lipid mixing.

Fluorescence measurements of Rho-labeled peptides treated with proteinase K

Fluorescence experiments were performed by using Rho-labeled peptides. Fluorescence kinetics were obtained at room temperature, with excitation set at 530 nm (5 nm slit) and emission set at 580 nm (5 nm slits). A Rho-labeled TMD peptide was first added alone from a stock solution in DMSO (final concentration 1μM and a maximum of 0.025% (v/v) DMSO) to a dispersion of PC:Chol LUVs (100 μM) in PBS, followed by the addition of proteinase K (24μg, from T. album, Sigma-Aldrich, St Louis, MO, USA). In a second experiment, a Rho-labeled TMD peptide was added to the vesicles together with unlabeled FP 1–33 (4μM), then left for 5 minutes to equilibrate. Enzyme was then added to allow cleavage of the peptide and the release of labeled short fragments to the solution.

Virus infectivity assay

Fully infectious HIV-1 HXBc2 concentrated virus stock was a kind gift from the AIDS Vaccine Program, SAIC. The infectivity of HIV-1 HXBc2 was determined using the TZM-bl cell line as a reporter. Cells were added (2×10^4 cells/well) to a 96-well clear-bottomed microtiter plate with 10% serum supplemented DMEM. Plates were incubated at 37°C for 18–24 hours to allow the cells to adhere. The media were then aspirated from each well and replaced with serum-free DMEM containing 40μg/mL DEAE-dextran. Stock dilutions of each peptide were prepared in DMSO so that each final concentration was achieved with 1% dilution. Upon addition of the peptides, the virus was added to the cells diluted in serum-free DMEM and containing 40 micrograms/mL DEAE-dextran. The plate was then incubated at 37°C for 18 hours to allow the infection to occur. Luciferase (Luc) activity was analyzed using the Steady-Glo Luciferase assay kit (Promega, Madison, WI). The Luc gene is under the transcriptional control of the Nef promoter. Therefore, Luc is expressed in the target cells only upon infection. Inhibition was calculated as Luc expression levels of infected cells in the presence of the indicated peptides divided by the expression levels in the absence of the peptide (taken as 100% infection).

Accession numbers

UniProtKB: **P04578** – HIV-1 Envelope glycoprotein gp160 (HXB2 strain)

RESULTS

The GxxxG motif is important for self-assembly of the gp41 TMD and not for association with FP

Synthetic peptides and their corresponding ToxR constructs were prepared to include regions derived from gp41 TMD. This sequence contains the two motifs of interest: the GxxxG and the GLRI motifs. Mutations were done to disrupt each motif separately (Table 1). In order to investigate whether the TMD, and specifically its GxxxG motif, contributes to the self-assembly of gp41 and to the hetero association with FP, we utilized the ToxR assay (47). The ToxR system is composed of three different components, the MalE recognition of maltose, the TMD of interest, and a functional ToxR transcription factor that operates as a dimer. Dimerization of the ToxR is triggered by the interactions of the selected TMDs and when an association occurs the LacZ gene is specifically transcribed. This method is used to assess the degree of association of a given transmembrane sequence. Utilizing the ToxR system, we measured the extent of association of the three constructs listed in Table 1. Note that substitution of Gly or Arg within the gp41 TMD to Ile, leads to impaired self-assembly in a TOXCAT assay (52). In addition, recent molecular dynamic simulations revealed that

the GxxxG motif can stabilize not only dimers but also trimers (52). All assays were performed in comparison to Glycophorin A (GpA) TMD, which is well known for its ability to form homo dimmers, as well as a TMD sequence of A15 (15 Ala residues), which served as a negative control (53–56). The data revealed that eliminating the GxxxG motif abolishes the ability of the TMD to self-associate within the membrane (Figure 2A, GGG construct). Interestingly, mutating Arg to Glu within the GLRI motif, thus introducing a negative charge to the sequence, improved significantly the ability of the mutant to self-associate (Figure 2A, R2E construct). The finding that the presence of Glu elevates the level of association within the membrane has been documented for other TMDs such as the aspartate and ErbB receptors (57–60). The expression levels of the constructs were measured to ensure that the differences are not related to changes in the expression of the constructs (Figure 2B). To further evaluate the ability of FP to associate with TMD, we performed competition assays between the TMD sequences and exogenously added synthetic FP peptide (Figure 2C). In this assay the association between the added peptide and the TMD within the ToxR leads to decreased LacZ transcription due to interference with the association within the membrane. Note that we did not assay the ability of FP and the GGG construct to associate owing to the very low initial level of self-assembly of GGG (Figure 2A). The data reveal that both the WT and R2E TMDs associate with FP. In contrast, when FP was added to a GpA TMD plasmid no decrease in LacZ was observed, supporting a specific association between FP and the TMDs (Figure 2C). The observed association between FP and the R2E mutant may be due to the presence of the GxxxG motif in both peptides or the presence of a Arg residue within the FP sequence.

Gp41 TMD interacts with gp41 FP independently of the GxxxG motif

To further verify that FP and TMD associate with each other, we performed a Fluorescence Resonance Energy Transfer (FRET) assay between NBD-FP (1–33) (fluorescence donor) and Rho-TMD (fluorescent acceptor) when bound to PC:Chol LUVs. The wavelength of the maximal emission energy of NBD when it is in a hydrophobic environment is 525–530nm, and it overlaps with the excitation spectra of Rho. The FRET method is based on the close association of two moieties (R_0=51Å) thus allowing energy to transfer from one to the other. The emission maxima of Rho is detected at 575–580nm (the emission spectra of the different peptides alone are presented in Figure S1). The FRET data revealed a significant association between FP (1–33) and the different analogs of the TMD (Figure 3A–C and Figure S2), with a direct correlation to their ability to self-assemble. This is evident by the decrease in emission intensity detected at 525–530nm. A control peptide, the TMD of the Tar receptor, exhibited significantly lower FRET with FP (Figure 3D). Importantly, the interaction between FP and TMD does not depend on the GxxxG motif. Note that the lack of increased signal at 580 nm observed for the R2E mutant is possibly due to the strong self-association of this peptide which in this case can lead to a quenching effect. This falls in line with the results seen for WT and GGG, which in both there is a correlation between the level of self-association and the increase at 580nm. The WT peptide which showed intermediate levels of self-association showed median levels of increase. In order to verify that the associations detected are through membrane-bound peptides and not via aggregation in the solution, we established titration curves (Figure S3) for all three TMD peptides (for FP titration curves see (61)). The extrapolated Kd values for each peptide are as follows: WT- $(2.7\pm1.2)\times10^{-5}$ M^{-1}; R2E- $(2.4\pm1.1)\times10^{-5}$ M-1; and GGG- $(1.6\pm0.6)\times10^{-5}$ M^{-1}. These data revealed that at a peptide:lipid ratio of 1:8000 (the initial ratio used in the FRET assay) all the peptides added are associated with the LUVs.

Binding of FP to gp41 TMD protects it from rapid enzymatic degradation

To determine whether the association of FP and TMD can lead to their re-organization when bound to membranes, we used an enzymatic degradation assay. For this purpose, we added

Rho-labeled TMD (Rho-TMD) to a solution of LUVs and measured the fluorescence at 580nm. We then added proteinase K and monitored the kinetics of peptide degradation, indicated by an increase in the Rho fluorescence. Figure 4a shows a rapid increase in the fluorescence above the initial level after the addition of proteinase K. The addition of FP to Rho-TMD prior to the addition of proteinase K resulted in slower kinetics of cleavage to a level significantly below the initial fluorescence (Figure 4a dashed line). This suggests that the association of FP and TMD results in a protecting effect from the cleavage by the enzyme owing to a change in the location/organization of the TMD peptide within the membrane bilayers. We used as a negative control Rho-labeled LL37, a well-studied membrane-bound antimicrobial peptide. Figure 4b shows that the addition of FP to LL37 did not alter the kinetics of degradation or the overall intensity of the freed Rho.

Lipid mixing induced by gp41 TMD and its mutants is enhanced by FP

Previous mutation/deletion studies with intact gp41 indicated a role for the TMD in membrane fusion (37, 62–64). However, it is not clear whether these mutations affected the ability of this region to participate in the actual fusion event or other processes such as proper assembly within the membrane. To address this question, we performed lipid mixing assays with the TMD peptides using PC:Chol LUVs. The lipid mixing activities of the TMD and its mutants alone are shown in Figure 5 (white squares). In addition, negative-staining electron microscopy was used to visualize membrane fusion (data not shown). Overall, the data revealed that the TMD and its two mutants have similar and significant dose-dependent lipid mixing activity when applied alone. In order to verify that the effects observed are specific to gp41 TMD peptides, we used the TAR1 TMD peptide as a negative control (65). The lipid mixing activity of Tar-1 was less than 1% and therefore is not shown in Figure 5.

FP can also induce membrane fusion when applied alone (66, 67). Here we showed that it binds the TMD within the membrane milieu (Figure 3). It was therefore interesting to examine whether a mixture of FP and TMD can enhance their lipid mixing ability. To this end, we performed a lipid mixing assay in which we used FP and TMD either alone or in combinations. In these experiments, cooperation between the peptides was determined when the lipid mixing of the mixture was higher than the calculated sum of each peptide when used alone. The data are summarized in Figures 5a, 5b, and 5c for the WT-TMD, GGG, and R2E mutants, respectively. The data clearly indicate that in the lower peptide:lipid molar ratios, the lipid mixing activity significantly increased upon combining the FP and TMD peptides. This is in agreement with the ability of FP to associate with the three TMDs (Figure 4).

The TMD and FP peptides inhibit HIV-1 virus - cell fusion

In light of the association observed between the FP and TMD peptides and their effect on the direct lipid mixing process of phospholipid membranes, we investigated their effect on the fusion between intact HIV-1 virions and target cells. These target cells contain Luciferase expression plasmids that are inducible by viral transcription factors. Therefore, only infected cells express Luciferase. The data, shown in Figure 6, revealed that all four peptides, namely, FP, WT, R2E, and GGG, are inhibitors to some extent, and that FP is the most active one. Thus, the TMD peptide can directly influence the *in-vitro* fusion induced by intact HIV-1 virus. Similarly to other peptides derived from gp41, it is reasonable to assume that the exogenous FP and TMD peptides interfere with the proper assembly of the endogenous FP and TMDs within the intact virus, by associating with their counterparts.

Exogenous TMDs destabilize the association of WT TMD independent of the GxxxG motif

The ability of the TMD peptides to inhibit virus-cell fusion could be due to their interaction with FP and/or with the endogenous TMD segment. In order to assess the ability of the

peptides to associate with endogenous TMD within native membranes, we performed competition experiments with exogenously added synthetic TMD peptides using the ToxR-TM-MalE (WT) construct. The data revealed that both WT and its mutated peptides were able to associate with the WT construct (Figure 7). Note that the GGG mutant could hetero-associate with the WT TMD, even though it could not homo-associate under similar experimental conditions owing to the absence of the GxxxG dimerization motif (Figure 2).

DISCUSSION

This study reports several important findings regarding the possible functional contribution of the TMD to the fusion process: (i) The TMD self-associates in the membrane via the GxxxG motif and hetero-associates with FP via the C-terminal TMD containing the GLRI motif; (ii) Peptides derived from TMD induce lipid mixing; (iii) TMD peptides inhibit native virus-cell fusion, and (iv) Hetero-association between FP and TMD leads to enhanced lipid mixing. These findings will be discussed with respect to the contribution of the TMD to the membrane fusion event.

TMD self-assembly

Many studies have demonstrated the significance of the association between transmembrane domains of various membrane proteins for their function (27, 29, 32, 33, 43, 55, 68). This assembly is driven by several motifs, among which GxxxG is the most studied one. Current data suggest a role for the GxxxG motif in virus replication, proper intracellular trafficking, self-assembly, and fusion kinetics, but no direct correlation has been reported between gp41 TMD self/hetero-association and its fusion activity (38, 52, 69, 70). Here we show that the GxxxG motif of TMD is crucial for it's self-assembly (Figure 1A, GGG), Nevertheless, mutation of Arg at position 694 to Glu significantly enhanced the self-association of the TMD (Figure 1A R2E). This is in line with studies showing that a Glu within TMDs enhances their assembly (58, 65, 71, 72). However, a GxxxG mutated TMD peptide can hetero-associate with the WT TMD (Figure 7).

TMD hetero association

The TMD of gp41 is highly conserved among HIV-1 strains and the Arg within the TMD is highly conserved even among HIV-2 strains (73). The appearance of charged amino acids within the membrane is relatively rare. Nevertheless, ionic interactions can occur within membranes and enhance association (65, 72). For example, mutations in the association motif within the TMD of the Tar receptor, in which a negatively charged amino acid (Glu) was incorporated, significantly increased the self-association of the TMD. On the other hand, mutations to Arg at the same positions eliminated the assembly (29, 65). It has been suggested that Glu is not charged in the membrane environment; thus, two glutamic acids can create interhelical hydrogen bonds that eventually stabilize the dimeric form (65). All together, this may explain the observed enhancement of self-assembly reported here for the R2E mutant, and its ability to hetero-associate with the WT TMD. Its association with FP within the membrane environment can be driven by hydrogen bonds too, or by ionic interactions (E-R) when studied under other conditions. Importantly, although the ability of the R2E mutant to hetero-assemble with FP was maintained, its inhibitory function was decreased significantly, suggesting a role for arginine in the function of the protein.

HIV-1 is well known for its high rate of mutations. Although many regions in the viral genome are highly prone to mutations, each functional protein has highly conserved regions. Assuming that the main function of gp41 TMD lies in its contribution to the assembly of gp41, one would expect to find strains harboring the R2E mutation, thus improving gp41 homo-association. However, the fact that no such strains have been reported, together with

its conservation among HIV-1 and HIV-2, indicates that the GLRI motif is otherwise critical. This motif appears to allow the TMD enough “flexibility” to exchange its association partners from self-association to hetero-association with FP and/or additional proteins.

Gp41 TMD induces lipid mixing and associates with FP

Studies focusing on the contribution of gp41 TMD to the fusion process were done in the context of the intact protein (13, 34, 35, 64). These studies showed that the TMD affects the fusion process. A particular importance was ascribed to the GxxxG motif. To distinguish between the impact of a mutation on the proper assembly of gp41 and the effect on its direct contribution to the fusion process, we synthesized and studied peptides corresponding to the TMD and its mutants. These mutations interfered with two motifs: the GxxxG motif and the GLRI motif (Table 1). Here, lipid mixing assays demonstrated that TMD directly induces lipid mixing (Figure 5). The finding that the GGG peptide preserves fusogenic capacity is in line with studies done with the intact protein showing that mutating the GxxxG motif influences the kinetics of the fusion process but does not abolish it (64). In addition, the finding that the GGG mutant can only marginally self-associates within the membrane (Figure 2) suggests that TMD assembly is not a prerequisite for inducing membrane fusion.

To demonstrate the association between TMD and the FP peptides, we performed *in vivo* ToxR competition assays in bacteria and FRET assays in model liposomes (Figures 2C and 3, respectively). These assays showed that there is a significant association between the peptides in model liposomes, which is independent of the GxxxG motif (Figure 3B). Note that the GGG mutant can only slightly self-associate, as detected by the ToxR assay, whereas the WT and the R2E could self-associate dramatically. The slight homo-association of the GGG peptide can explain the highest increase in the emission of the acceptor at 580nm compared with the WT and the R2E mutant, in which their homo-association apparently causes quenching of the acceptor fluorescence at 580nm. It is evident from the ToxR assays that also in intact membranes FP can associate specifically with the TMD sequences and not with the GpA TMD sequence (Figure 2C). We also performed titration assays to verify that the peptides fully adhere to the liposomes at our assay ratios. Indeed, all three peptides strongly interact with the liposomes, with Kd values of 10^{-5}-$10^{-4}M^{-1}$.

Recently, we have shown that gp41 FP associates with the TMD of the α subunit of the T-cell receptor (TCR-α) via the GLRI motif, and that the same motif exists in the TMD of HIV (23, 24, 74, 75). This supports our findings of the association between FP and TMD of gp41. The ability of the R2E mutant TMD peptide to associate with FP, although to a lesser extent, is possibly due to the contribution of the GxxxG motif, which was preserved in this peptide, together with the GxxxG motif in FP (GSTMG). In addition, Glu in the R2E-TMD peptide can form hydrogen bonds with Arg in FP. Importantly; the association between FP and all three TMD peptides appears to be functionally important since it leads to an enhancement of their ability to induce lipid mixing (Figure 5). Our data further suggest that the enhanced fusion induced by mixing the two peptides is accompanied by a change in the location/organization of TMD upon its association with FP (Figure 4). The proximity between FP and TMD is further supported by the finding that the monoclonal antibody 2F5 binds to its target, the gp41 membrane proximal region (MPER), when it is associated with the elicited gp41 fusion peptide proximal region (FPPR) (21).

TMD peptides inhibit virus-cell fusion

There is an ongoing attempt to identify new HIV-1 entry inhibitors. Potent inhibitors originated from peptides derived from various regions within gp41 ectodomain. Of these inhibitors, the most studied is T20, also termed DP178 or Fuseon (reviewed in (17, 76, 77)).

These inhibitors interfere with the functional organization of gp41 during the ongoing fusion process. However, currently there is increasing evidence that new strains evolved with increasing resistance to T20. Since we have shown that FP can bind to the TMD (Figure 3 and 4) and that their co-incubation results in an enhanced lipid mixing (Figure 5), we examined the ability of each individual peptide to interfere with the virus-cell fusion process. The data reveal that the peptides inhibit virus-cell fusion in a dose-dependent manner (Figure 6). FP exhibited the highest level of inhibition. This is in line with its ability to strongly associates with the TMD and with previous studies done with FP (61, 67, 78). The inhibitory concentrations of the TMD and FP are in the low μM concentration range. Besides T20 and its derivatives, a similar range of concentrations was reported for peptide inhibitors derived from the N terminal of gp41, namely, N17 and N23 (40, 79). The high conservation of the TMD sequence suggests that the occurrence of inhibitory escape mutations within it might be more difficult, compared with those that occurred in the extracellular domains of gp41.

Utilization of a common fusion mechanism in diverse systems

Our data are in line with the current concept suggesting that similarities exist between viral fusion and the SNARE fusion mechanisms (68, 80). These include the presence of heptad repeats in their sequences, the formation of helix bundles (4-helix bundles in SNAREs and 6-helix bundles in HIV) and coiled-coil structures. Previously, it has been suggested that the transmembrane segments of SNAREs are the equivalent of viral fusion peptides and are important for forming productive fusion. Therefore, their fusion mechanisms are likely to share crucial features with those of viral fusion (81–83). An interesting characteristic of SNAREs is the presence of a highly conserved Arg residue within the v-SNARE synaptobrevin, which fuses with cellular membranes. Additionally, it was shown in the case of the synaptobrevin/synaptophysin complex that the TMD of synaptobrevin is crucial for their association and apparently this is done by association with an N’ terminal segment from synaptophysin or one of its transmembrane segments (TMSs) (84). Moreover, the functional association between FP and TMD of viral envelope proteins is not the sole property of HIV-1. The HA protein of Influenza virus was shown to utilize this mechanism during its fusion process (43, 85). This may indicate that the fusion process, although not conserved at the sequence level between distinct viruses, is highly conserved mechanistically. This is in agreement with additional studies showing that enveloped viruses share many features regarding their fusion mechanism (86–90).

In summary, in this study we showed that gp41 FP is functionally associated with TMD. This led to an enhancement in their ability to induce lipid mixing of model membranes. Furthermore, peptides derived from the TMD and FP could inhibit virus-cell fusion, probably by interfering with the functional association of the parental endogenous regions. The data suggest that the TMD harbors two independent properties that are tightly regulated during the fusion process. The first is its homo-association which is governed by the GxxxG motif, and the second one is its hetero-association with FP.

Supplementary Material

Refer to Web version on PubMed Central for supplementary material.

Acknowledgments

This study was supported by the Israel Science Foundation (to YS) and in part by federal funds from the National Cancer Institute, the National Institutes of Health, under contract HHSN26120080001E (to RB). The content of this publication does not necessarily reflect the views or policies of the Department of Health and Human Services, nor does it mention any trade names, commercial products, or organizations or imply endorsement by the U.S.

Government. This research was supported in part by the Intramural Research Program of the NIH, National Cancer Institute, Center for Cancer Research (to RB).

Abbreviations

FP	fusion peptide
TMD	transmembrane domain
Env	envelope glycoprotein gp160
NHR	N' heptad repeat
CHR	C' heptad repeat
FRET	fluorescence resonance energy transfer
PHI	pre-hairpin
SHB	six helix bundle
MPER	membrane proximal external region
NBD	nitrobenzoxadiazole
Rho	Rhodamine
LUV	large unilamillar vesicle
PC	phosphatidyl choline
Chol	cholesterol
GpA	Glycophrin A
Luc	Luciferase

REFERENCES

1. Wyatt R, Sodroski J. The HIV-1 envelope glycoproteins: fusogens, antigens, and immunogens. Science. 1998; 280:1884–1888. [PubMed: 9632381]
2. Gallo SA, Finnegan CM, Viard M, Raviv Y, Dimitrov A, Rawat SS, Puri A, Durell S, Blumenthal R. The HIV Env-mediated fusion reaction. Biochim. Biophys. Acta. 2003; 1614:36–50. [PubMed: 12873764]
3. Weiss CD. HIV-1 gp41: mediator of fusion and target for inhibition. AIDS Rev. 2003; 5:214–221. [PubMed: 15012000]
4. Zhu P, Liu J, Bess J Jr, Chertova E, Lifson JD, Grise H, Ofek GA, Taylor KA, Roux KH. Distribution and three-dimensional structure of AIDS virus envelope spikes. Nature. 2006; 441:847–852. [PubMed: 16728975]
5. Chan DC, Kim PS. HIV entry and its inhibition. Cell. 1998; 93:681–684. [PubMed: 9630213]
6. Pierson TC, Doms RW. HIV-1 entry and its inhibition. Curr Top Microbiol Immunol. 2003; 281:1–27. [PubMed: 12932074]
7. Markovic I, Clouse KA. Recent advances in understanding the molecular mechanisms of HIV-1 entry and fusion: revisiting current targets and considering new options for therapeutic intervention. Curr HIV Res. 2004; 2:223–234. [PubMed: 15279586]
8. Kowalski M, Potz J, Basiripour L, Dorfman T, Goh WC, Terwilliger E, Dayton A, Rosen C, Haseltine W, Sodroski J. Functional regions of the envelope glycoprotein of human immunodeficiency virus type 1. Science. 1987; 237:1351–1355. [PubMed: 3629244]
9. Gomara MJ, Lorizate M, Huarte N, Mingarro I, Perez-Paya E, Nieva JL. Hexapeptides that interfere with HIV-1 fusion peptide activity in liposomes block GP41-mediated membrane fusion. FEBS Lett. 2006; 580:2561–2566. [PubMed: 16647705]

10. Dimitrov AS, Louis JM, Bewley CA, Clore GM, Blumenthal R. Conformational changes in HIV-1 gp41 in the course of HIV-1 envelope glycoprotein-mediated fusion and inactivation. Biochemistry. 2005; 44:12471–12479. [PubMed: 16156659]
11. Melikyan GB. Common principles and intermediates of viral protein-mediated fusion: the HIV-1 paradigm. Retrovirology. 2008; 5:111. [PubMed: 19077194]
12. Hughes A, Nelson M. HIV entry: new insights and implications for patient management. Curr Opin Infect Dis. 2009; 22:35–42. [PubMed: 19532079]
13. Liu J, Deng Y, Li Q, Dey AK, Moore JP, Lu M. Role of a putative gp41 dimerization domain in human immunodeficiency virus type 1 membrane fusion. J. Virol. 2010; 84:201–209. [PubMed: 19846514]
14. Debnath AK. Progress in identifying peptides and small-molecule inhibitors targeted to gp41 of HIV-1. Expert Opin Investig Drugs. 2006; 15:465–478.
15. Korazim O, Sackett K, Shai Y. Functional and Structural Characterization of HIV-1 gp41 Ectodomain Regions in Phospholipid Membranes Suggests that the Fusion-active Conformation Is Extended. J. Mol. Biol. 2006 Dec 15; 364(5):1103–1117. [PubMed: 17045292]
16. Yuan W, Bazick J, Sodroski J. Characterization of the multiple conformational States of free monomeric and trimeric human immunodeficiency virus envelope glycoproteins after fixation by cross-linker. J Virol. 2006; 80:6725–6737. [PubMed: 16809278]
17. Pang W, Tam SC, Zheng YT. Current peptide HIV type-1 fusion inhibitors. Antivir Chem Chemother. 2009; 20:1–18. [PubMed: 19794228]
18. Moreno MR, Guillen J, Perez-Berna AJ, Amoros D, Gomez AI, Bernabeu A, Villalain J. Characterization of the interaction of two peptides from the N terminus of the NHR domain of HIV-1 gp41 with phospholipid membranes. Biochemistry. 2007; 46:10572–10584. [PubMed: 17711304]
19. Pan C, Liu S, Jiang S. HIV-1 gp41 fusion intermediate: a target for HIV therapeutics. J Formos Med Assoc. 2010; 109:94–105. [PubMed: 20206833]
20. Cohen FS, Melikyan GB. The energetics of membrane fusion from binding, through hemifusion, pore formation, and pore enlargement. J Membr Biol. 2004; 199:1–14. [PubMed: 15366419]
21. Fiebig U, Schmolke M, Eschricht M, Kurth R, Denner J. Mode of interaction between the HIV-1-neutralizing monoclonal antibody 2F5 and its epitope. AIDS. 2009; 23:887–895. [PubMed: 19414989]
22. Buzon V, Natrajan G, Schibli D, Campelo F, Kozlov MM, Weissenhorn W. Crystal structure of HIV-1 gp41 including both fusion peptide and membrane proximal external regions. PLoS Pathog. 2010; 6:e1000880. [PubMed: 20463810]
23. Cohen T, Pevsner-Fischer M, Cohen N, Cohen IR, Shai Y. Characterization of the interacting domain of the HIV-1 fusion peptide with the transmembrane domain of the T-cell receptor. Biochemistry. 2008; 47:4826–4833. [PubMed: 18376816]
24. Cohen T, Cohen SJ, Antonovsky N, Cohen IR, Shai Y. HIV-1 gp41 and TCRalpha trans-membrane domains share a motif exploited by the HIV virus to modulate T-cell proliferation. PLoS Pathog. 2010; 6:e1001085. [PubMed: 20824090]
25. Op De Beeck A, Montserret R, Duvet S, Cocquerel L, Cacan R, Barberot B, Le Maire M, Penin F, Dubuisson J. The transmembrane domains of hepatitis C virus envelope glycoproteins E1 and E2 play a major role in heterodimerization. J. Biol. Chem. 2000; 275:31428–31437. [PubMed: 10807921]
26. Tatulian SA, Tamm LK. Secondary structure, orientation, oligomerization, and lipid interactions of the transmembrane domain of influenza hemagglutinin. Biochemistry. 2000; 39:496–507. [PubMed: 10642174]
27. Curran AR, Engelman DM. Sequence motifs, polar interactions and conformational changes in helical membrane proteins. Curr Opin Struct Biol. 2003; 13:412–417. [PubMed: 12948770]
28. Nayak DP, Hui EK, Barman S. Assembly and budding of influenza virus. Virus Res. 2004; 106:147–165. [PubMed: 15567494]
29. Sal-Man N, Gerber D, Shai Y. The identification of a minimal dimerization motif QXXS that enables homo- and hetero-association of transmembrane helices in vivo. J. Biol. Chem. 2005; 280:27449–27457. [PubMed: 15911619]

30. Shai Y. Molecular recognition between membrane-spanning polypeptides. Trends Biochem. Sci. 1995; 20:460–464. [PubMed: 8578589]
31. Ng DP, Deber CM. Modulation of the oligomerization of myelin proteolipid protein by transmembrane helix interaction motifs. Biochemistry. 2010; 49:6896–6902. [PubMed: 20695528]
32. Senes A, Engel DE, DeGrado WF. Folding of helical membrane proteins: the role of polar, GxxxG-like and proline motifs. Curr. Opin. Struct. Biol. 2004; 14:465–479. [PubMed: 15313242]
33. Johnson RM, Rath A, Deber CM. The position of the Gly-xxx-Gly motif in transmembrane segments modulates dimer affinity. Biochem. Cell. Biol. 2006; 84:1006–1012. [PubMed: 17215886]
34. Miyauchi K, Komano J, Yokomaku Y, Sugiura W, Yamamoto N, Matsuda Z. Role of the specific amino acid sequence of the membrane-spanning domain of human immunodeficiency virus type 1 in membrane fusion. J Virol. 2005; 79:4720–4729. [PubMed: 15795258]
35. Yue L, Shang L, Hunter E. Truncation of the membrane-spanning domain of human immunodeficiency virus type 1 envelope glycoprotein defines elements required for fusion, incorporation, and infectivity. J. Virol. 2009; 83:11588–11598. [PubMed: 19726514]
36. Shang L, Yue L, Hunter E. Role of the membrane-spanning domain of human immunodeficiency virus type 1 envelope glycoprotein in cell-cell fusion and virus infection. J. Virol. 2008; 82:5417–5428. [PubMed: 18353944]
37. Kondo N, Miyauchi K, Meng F, Iwamoto A, Matsuda Z. Conformational changes of the HIV-1 envelope protein during membrane fusion are inhibited by the replacement of its membrane-spanning domain. J Biol Chem. 2010; 285:14681–14688. [PubMed: 20197275]
38. Long Y, Meng F, Kondo N, Iwamoto A, Matsuda Z. Conserved arginine residue in the membrane-spanning domain of HIV-1 gp41 is required for efficient membrane fusion. Protein Cell. 2010; 2:369–376. [PubMed: 21667332]
39. He Y, Cheng J, Li J, Qi Z, Lu H, Dong M, Jiang S, Dai Q. Identification of a critical motif for the human immunodeficiency virus type 1 (HIV-1) gp41 core structure: implications for designing novel anti-HIV fusion inhibitors. J. Virol. 2008; 82:6349–6358. [PubMed: 18417584]
40. Ashkenazi A, Shai Y. Insights into the mechanism of HIV-1 envelope induced membrane fusion as revealed by its inhibitory peptides. Eur Biophys J. 2011 Apr; 40(4):349–357. [PubMed: 21258789]
41. Maddox MW, Longo ML. Conformational partitioning of the fusion peptide of HIV-1 gp41 and its structural analogs in bilayer membranes. Biophys J. 2002; 83:3088–3096. [PubMed: 12496080]
42. Blumenthal R, Dimitrov DS. Targeting the sticky fingers of HIV-1. Cell. 2007; 129:243–245. [PubMed: 17448985]
43. Chang DK, Cheng SF, Kantchev EA, Lin CH, Liu YT. Membrane interaction and structure of the transmembrane domain of influenza hemagglutinin and its fusion peptide complex. BMC Biol. 2008; 6:2. [PubMed: 18197965]
44. Melnyk RA, Partridge AW, Deber CM. Retention of native-like oligomerization states in transmembrane segment peptides: application to the Escherichia coli aspartate receptor. Biochemistry. 2001; 40:11106–11113. [PubMed: 11551208]
45. Rapaport D, Peled R, Nir S, Shai Y. Reversible surface aggregation in pore formation by pardaxin. Biophys J. 1996; 70:2502–2512. [PubMed: 8744290]
46. Liu F, Lewis RN, Hodges RS, McElhaney RN. Effect of variations in the structure of a polyleucine-based alpha-helical transmembrane peptide on its interaction with phosphatidylethanolamine Bilayers. Biophys J. 2004; 87:2470–2482. [PubMed: 15454444]
47. Langosch D, Brosig B, Kolmar H, Fritz HJ. Dimerisation of the glycophorin A transmembrane segment in membranes probed with the ToxR transcription activator. J Mol Biol. 1996; 263:525–530. [PubMed: 8918935]
48. Kolmar H, Frisch C, Kleemann G, Gotze K, Stevens FJ, Fritz HJ. Dimerization of Bence Jones proteins: linking the rate of transcription from an Escherichia coli promoter to the association constant of REIV. Biol Chem Hoppe Seyler. 1994; 375:61–70. [PubMed: 8003258]
49. Rapaport D, Shai Y. Interaction of fluorescently labeled pardaxin and its analogues with lipid bilayers. J Biol Chem. 1991; 266:23769–23775. [PubMed: 1748653]

50. Frey S, Tamm LK. Membrane insertion and lateral diffusion of fluorescence-labelled cytochrome c oxidase subunit IV signal peptide in charged and uncharged phospholipid bilayers. Biochem J. 1990; 272:713–719. [PubMed: 2176475]
51. Struck DK, Hoekstra D, Pagano RE. Use of resonance energy transfer to monitor membrane fusion. Biochemistry. 1981; 20:4093–4099. [PubMed: 7284312]
52. Kim JH, Hartley TL, Curran AR, Engelman DM. Molecular dynamics studies of the transmembrane domain of gp41 from HIV-1. Biochim. Biophys. Acta. 2009; 1788:1804–1812. [PubMed: 19540828]
53. Lemmon MA, Flanagan JM, Hunt JF, Adair BD, Bormann BJ, Dempsey CE, Engelman DM. Glycophorin A dimerization is driven by specific interactions between transmembrane alpha-helices. J Biol Chem. 1992; 267:7683–7689. [PubMed: 1560003]
54. Gerber D, Sal-Man N, Shai Y. Structural adaptation of the glycophorin A transmembrane homodimer to D-amino acid modifications. J Mol Biol. 2004; 339:243–250. [PubMed: 15123435]
55. Cuthbertson JM, Bond PJ, Sansom MS. Transmembrane helix-helix interactions: comparative simulations of the glycophorin a dimer. Biochemistry. 2006; 45:14298–14310. [PubMed: 17128969]
56. Anbazhagan V, Schneider D. The membrane environment modulates self-association of the human GpA TM domain-Implications for membrane protein folding and transmembrane signaling. Biochim Biophys Acta. 2010; 1798:1899–1907. [PubMed: 20603102]
57. Surratt CK, Johnson PS, Moriwaki A, Seidleck BK, Blaschak CJ, Wang JB, Uhl GR. -mu opiate receptor. Charged transmembrane domain amino acids are critical for agonist recognition and intrinsic activity. J Biol Chem. 1994; 269:20548–20553. [PubMed: 8051154]
58. Gratkowski H, Lear JD, DeGrado WF. Polar side chains drive the association of model transmembrane peptides. Proc Natl Acad Sci U S A. 2001; 98:880–885. [PubMed: 11158564]
59. Sal-Man N, Gerber D, Shai Y. The composition rather than position of polar residues (QxxS) drives aspartate receptor transmembrane domain dimerization in vivo. Biochemistry. 2004; 43:2309–2313. [PubMed: 14979727]
60. Mineev KS, Bocharov EV, Pustovalova YE, Bocharova OV, Chupin VV, Arseniev AS. Spatial structure of the transmembrane domain heterodimer of ErbB1 and ErbB2 receptor tyrosine kinases. J. Mol. Biol. 2010; 400:231–243. [PubMed: 20471394]
61. Kliger Y, Aharoni A, Rapaport D, Jones P, Blumenthal R, Shai Y. Fusion peptides derived from the HIV type 1 glycoprotein 41 associate within phospholipid membranes and inhibit cell-cell Fusion. Structure-function study. J Biol Chem. 1997; 272:13496–13505. [PubMed: 9153194]
62. Helseth E, Olshevsky U, Gabuzda D, Ardman B, Haseltine W, Sodroski J. Changes in the transmembrane region of the human immunodeficiency virus type 1 gp41 envelope glycoprotein affect membrane fusion. J. Virol. 1990; 64:6314–6318. [PubMed: 2243396]
63. Jacobs A, Garg H, Viard M, Raviv Y, Puri A, Blumenthal R. HIV-1 envelope glycoprotein-mediated fusion and pathogenesis: implications for therapy and vaccine development. Vaccine. 2008; 26:3026–3035. [PubMed: 18242797]
64. Shang L, Hunter E. Residues in the membrane-spanning domain core modulate conformation and fusogenicity of the HIV-1 envelope glycoprotein. Virology. 2010; 404:158–167. [PubMed: 20605619]
65. Sal-Man N, Shai Y. Arginine mutations within a transmembrane domain of Tar, an Escherichia coli aspartate receptor, can drive homodimer dissociation and heterodimer association in vivo. Biochem J. 2005; 385:29–36. [PubMed: 15330757]
66. Mobley PW, Lee HF, Curtain CC, Kirkpatrick A, Waring AJ, Gordon LM. The amino-terminal peptide of HIV-1 glycoprotein 41 fuses human erythrocytes. Biochim Biophys Acta. 1995; 1271:304–314. [PubMed: 7605797]
67. Buzon V, Padros E, Cladera J. Interaction of fusion peptides from HIV gp41 with membranes: a time-resolved membrane binding, lipid mixing, and structural study. Biochemistry. 2005; 44:13354–13364. [PubMed: 16201760]
68. Martens S, McMahon HT. Mechanisms of membrane fusion: disparate players and common principles. Nat Rev Mol Cell Biol. 2008; 9:543–556. [PubMed: 18496517]

69. Hernandez LD, Hoffman LR, Wolfsberg TG, White JM. Virus-cell and cell-cell fusion. Annu. Rev. Cell. Dev. Biol. 1996; 12:627–661. [PubMed: 8970739]
70. Miyauchi K, Curran AR, Long Y, Kondo N, Iwamoto A, Engelman DM, Matsuda Z. The membrane-spanning domain of gp41 plays a critical role in intracellular trafficking of the HIV envelope protein. Retrovirology. 2010; 7:95. [PubMed: 21073746]
71. Weiner DB, Liu J, Cohen JA, Williams WV, Greene MI. A point mutation in the neu oncogene mimics ligand induction of receptor aggregation. Nature. 1989; 339:230–231. [PubMed: 2654648]
72. Moore DT, Berger BW, DeGrado WF. Protein-protein interactions in the membrane: sequence, structural, and biological motifs. Structure. 2008; 16:991–1001. [PubMed: 18611372]
73. Jadhav S, Tripathy S, Kulkarni S, Chaturbhuj D, Ghare R, Bhattacharya J, Paranjape R. Genetic Conservation in gp36 Transmembrane Sequences of Indian HIV Type 2 Isolates. AIDS Res Hum Retroviruses. 2011 Dec 27.(12):1337–1343. [PubMed: 21453135]
74. Quintana FJ, Gerber D, Kent SC, Cohen IR, Shai Y. HIV-1 fusion peptide targets the TCR and inhibits antigen-specific T cell activation. J. Clin. Invest. 2005; 115:2149–2158. [PubMed: 16007266]
75. Bloch I, Quintana FJ, Gerber D, Cohen T, Cohen IR, Shai Y. T-cell inactivation and immunosuppressive activity induced by HIV gp41 via novel interacting motif. FASEB J. 2007; 21:393–401. [PubMed: 17185749]
76. Baldwin CE, Sanders RW, Berkhout B. Inhibiting HIV-1 entry with fusion inhibitors. Curr Med Chem. 2003; 10:1633–1642. [PubMed: 12871113]
77. Altmeyer R. Virus attachment and entry offer numerous targets for antiviral therapy. Curr Pharm Des. 2004; 10:3701–3712. [PubMed: 15579065]
78. Kliger Y, Gallo SA, Peisajovich SG, Munoz-Barroso I, Avkin S, Blumenthal R, Shai Y. Mode of action of an antiviral peptide from HIV-1. Inhibition at a post-lipid mixing stage. J. Biol. Chem. 2001; 276:1391–1397. [PubMed: 11027678]
79. Eckert DM, Kim PS. Design of potent inhibitors of HIV-1 entry from the gp41 N-peptide region. Proc Natl Acad Sci U S A. 2001; 98:11187–11192. [PubMed: 11572974]
80. Blumenthal R, Clague MJ, Durell SR, Epand RM. Membrane fusion. Chem Rev. 2003; 103:53–69. [PubMed: 12517181]
81. Jahn R, Sudhof TC. Membrane fusion and exocytosis. Annu Rev Biochem. 1999; 68:863–911. [PubMed: 10872468]
82. Sollner TH. Intracellular and viral membrane fusion: a uniting mechanism. Curr Opin Cell Biol. 2004; 16:429–435. [PubMed: 15261676]
83. Ungermann C, Langosch D. Functions of SNAREs in intracellular membrane fusion and lipid bilayer mixing. J Cell Sci. 2005; 118:3819–3828. [PubMed: 16129880]
84. Yelamanchili SV, Reisinger C, Becher A, Sikorra S, Bigalke H, Binz T, Ahnert-Hilger G. The C-terminal transmembrane region of synaptobrevin binds synaptophysin from adult synaptic vesicles. Eur J Cell Biol. 2005; 84:467–475. [PubMed: 15900706]
85. Skehel JJ, Wiley DC. Receptor binding and membrane fusion in virus entry: the influenza hemagglutinin. Annu Rev Biochem. 2000; 69:531–569. [PubMed: 10966468]
86. Weissenhorn W, Dessen A, Calder LJ, Harrison SC, Skehel JJ, Wiley DC. Structural basis for membrane fusion by enveloped viruses. Mol Membr Biol. 1999; 16:3–9. [PubMed: 10332732]
87. Colman PM, Lawrence MC. The structural biology of type I viral membrane fusion. Nat Rev Mol Cell Biol. 2003; 4:309–319. [PubMed: 12671653]
88. Jardetzky TS, Lamb RA. Virology: a class act. Nature. 2004; 427:307–308. [PubMed: 14737155]
89. MacCallum JL, Bennett WF, Tieleman DP. Partitioning of amino acid side chains into lipid bilayers: results from computer simulations and comparison to experiment. J Gen Physiol. 2007; 129:371–377. [PubMed: 17438118]
90. White JM, Delos SE, Brecher M, Schornberg K. Structures and mechanisms of viral membrane fusion proteins: multiple variations on a common theme. Crit Rev Biochem Mol Biol. 2008; 43:189–219. [PubMed: 18568847]

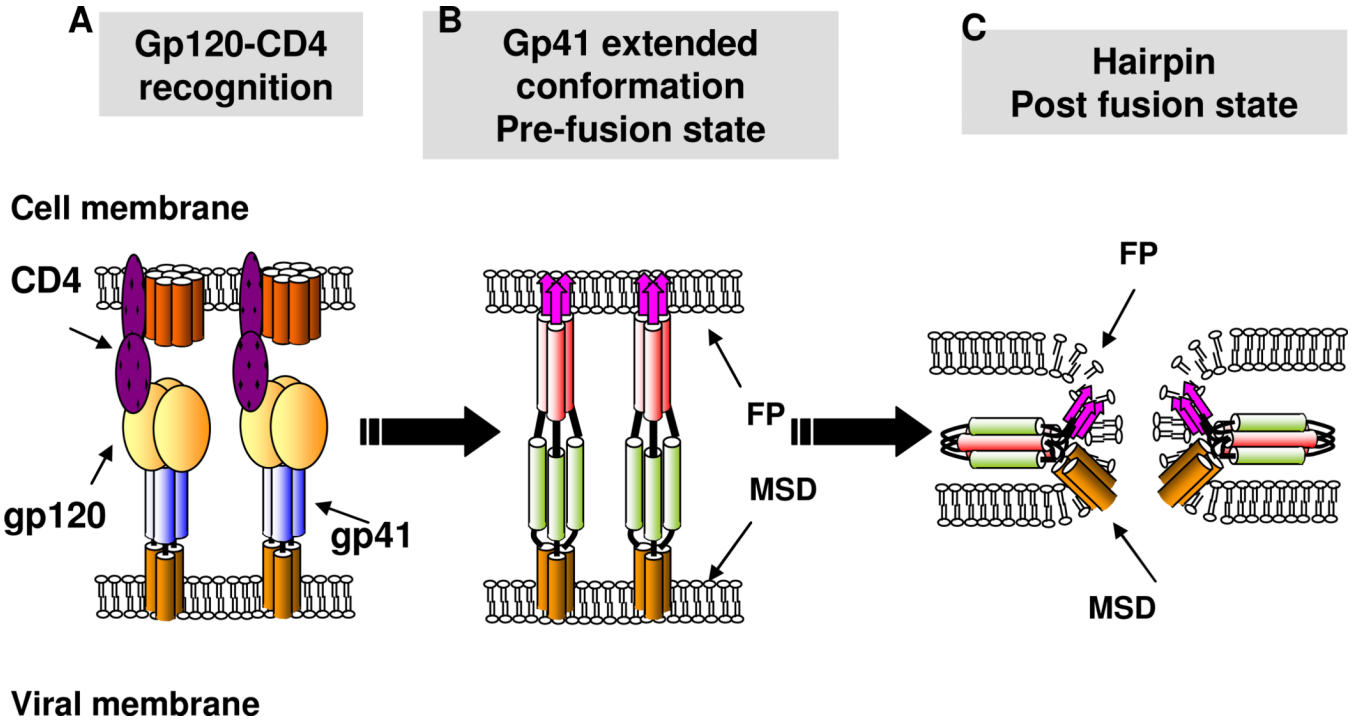

Figure 1. A schematic presentation of the gp41-induced fusion process

(A) The gp120 subunit of gp160 recognizes its corresponding receptor CD4 together with additional co receptors. This recognition leads to the separation of the non-covalently linked gp41 and the exposure of the fusion peptide. (B) The fusion peptide is inserted into the target cell membrane and the gp41 trimmer is reinforced. At this stage the structure is thought to be in an extended state. (C) After additional conformational changes a six-helix bundle is formed through interactions of the NHR and CHR and the two membranes are forced to be in proximity. Additional steps lead to full membrane mixing, resulting eventually in content mixing between the effector and target cells.

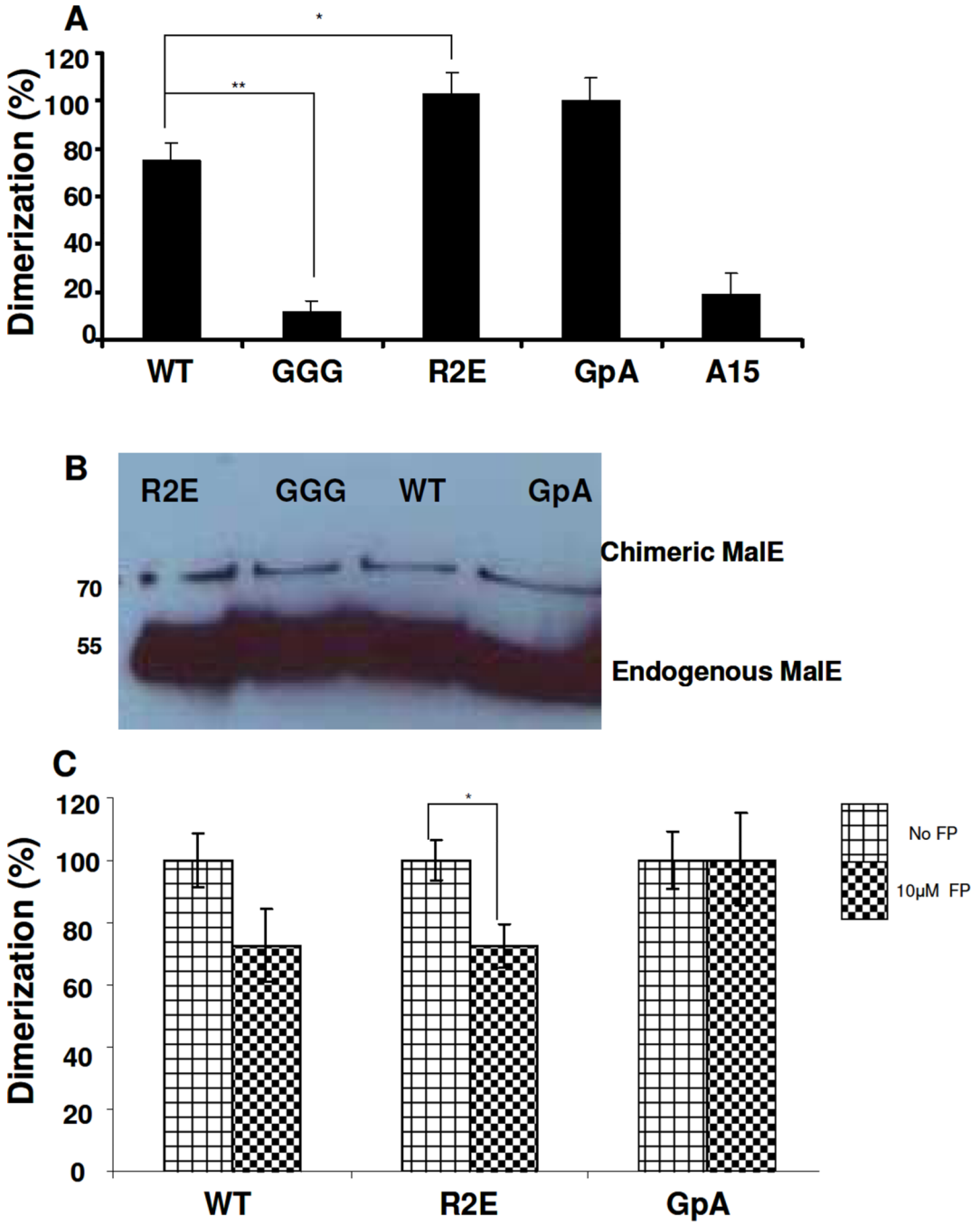

Figure 2. The GxxxG motif is critical for the ability of the TMD to homo-dimerize

(A) Cells expressing a ToxR-MalE chimera with the TMD sequences were examined for lacZ activity (normalized relative to the GpA sequence activity). All values are the average of at least three independent assays. Error bars represent the standard deviation. The exact sequences are indicated in Table 1. Statistical significance was calculated by a student T-test (P values - * ≤ 0.01, ** ≤ 0.001.) (B) Comparison of the ToxR-TM-MalE chimera proteins' expression levels (70kDa). Samples of FHK12 cells containing the different sequences of gp41 TMD within the ToxR-MalE chimera protein were lysed in sodium dodecyl sulfate-sample buffer, separated on 12% SDS-PAGE, and then immunoblotted using anti-MBP antibody (New England Biolabs). Sizes are indicated in kDa on the right. (C) Bacteria

expressing the indicated constructs were grown alone (white boxes) or in the presence of 10μM FP (1–33) (black boxes). The LacZ expression levels were evaluated and the values were compared to the expression of LacZ in the absence of the exogenous peptide.

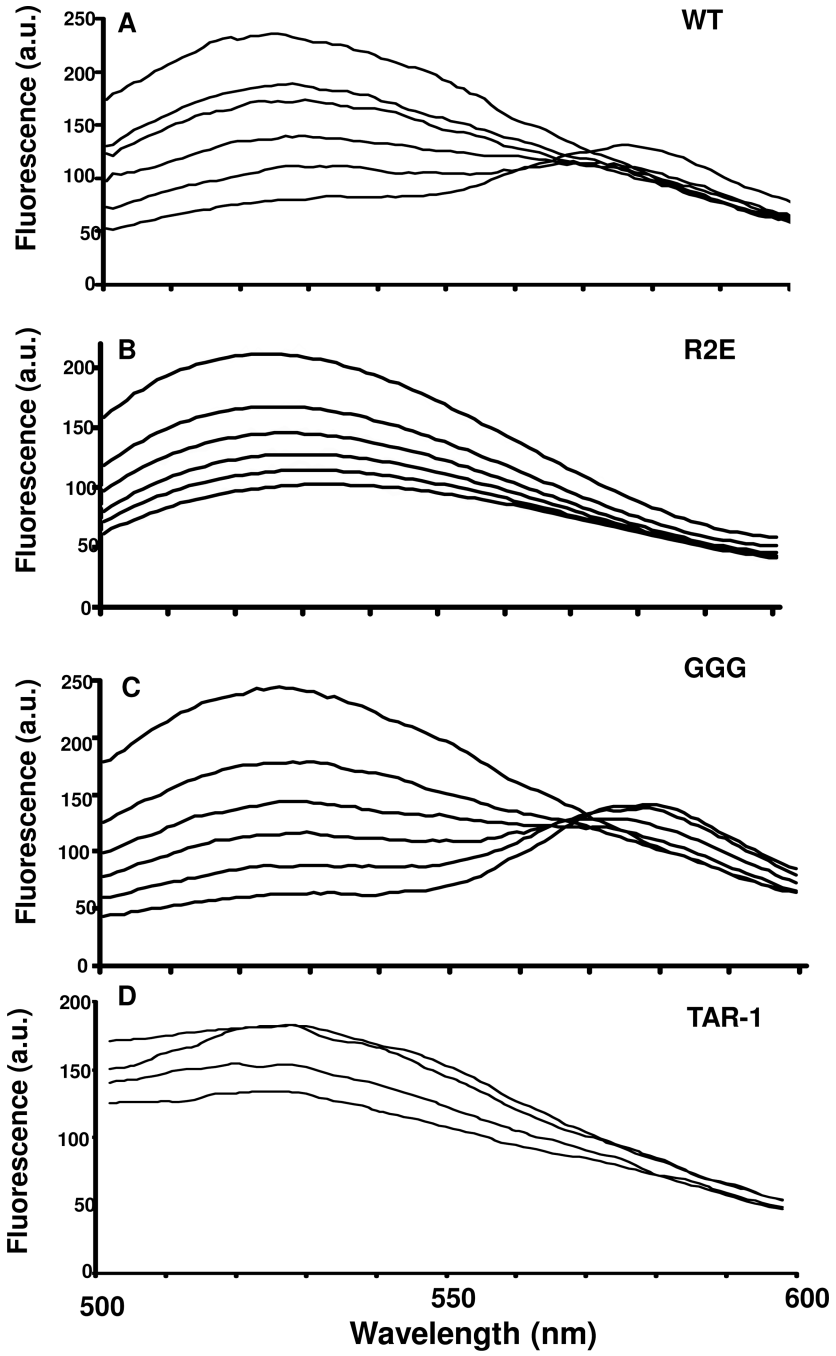

Figure 3. Fluorescence Energy Transfer (FRET) measurements between gp41 TMD and gp41 FP

Fluorescence spectra were obtained at room temperature, with excitation set at 467 nm (5-nm slit) and an emission scan at 500–600 nm (10-nm slits). NBD-labeled FP peptide was added first from a stock solution in DMSO (final concentration 0.4 μM and a maximum of 0.25% (v/v) DMSO) to a dispersion of PC:Chol LUV (100 μM) in PBS. This was followed by the addition of the following: A- Rho-labeled gp41 TMD-WT peptide, B- Rho-labeled gp41 TMD-GGG and C- Rho-labeled gp41 TMD-R2E, all in sequential doses ranging from 0.0125 μM to 0.2 μM (stock in DMSO), generating a ratio of 1:32, 1:16, 1:8, 1:4, and 1:2 Rho-NBD presented from top to bottom. In all graphs the upper spectrum represents the emission of the NBD- labeled peptide alone. Fluorescence spectra were obtained before and

after addition of the Rho-labeled peptide. The fluorescence values were corrected by subtracting the corresponding blank (buffer with the same vesicle concentration alone). D-An acceptor control peptide – Rho-TAR1-TM – was tested with NBD-FP to demonstrate the specificity of the energy transfer.

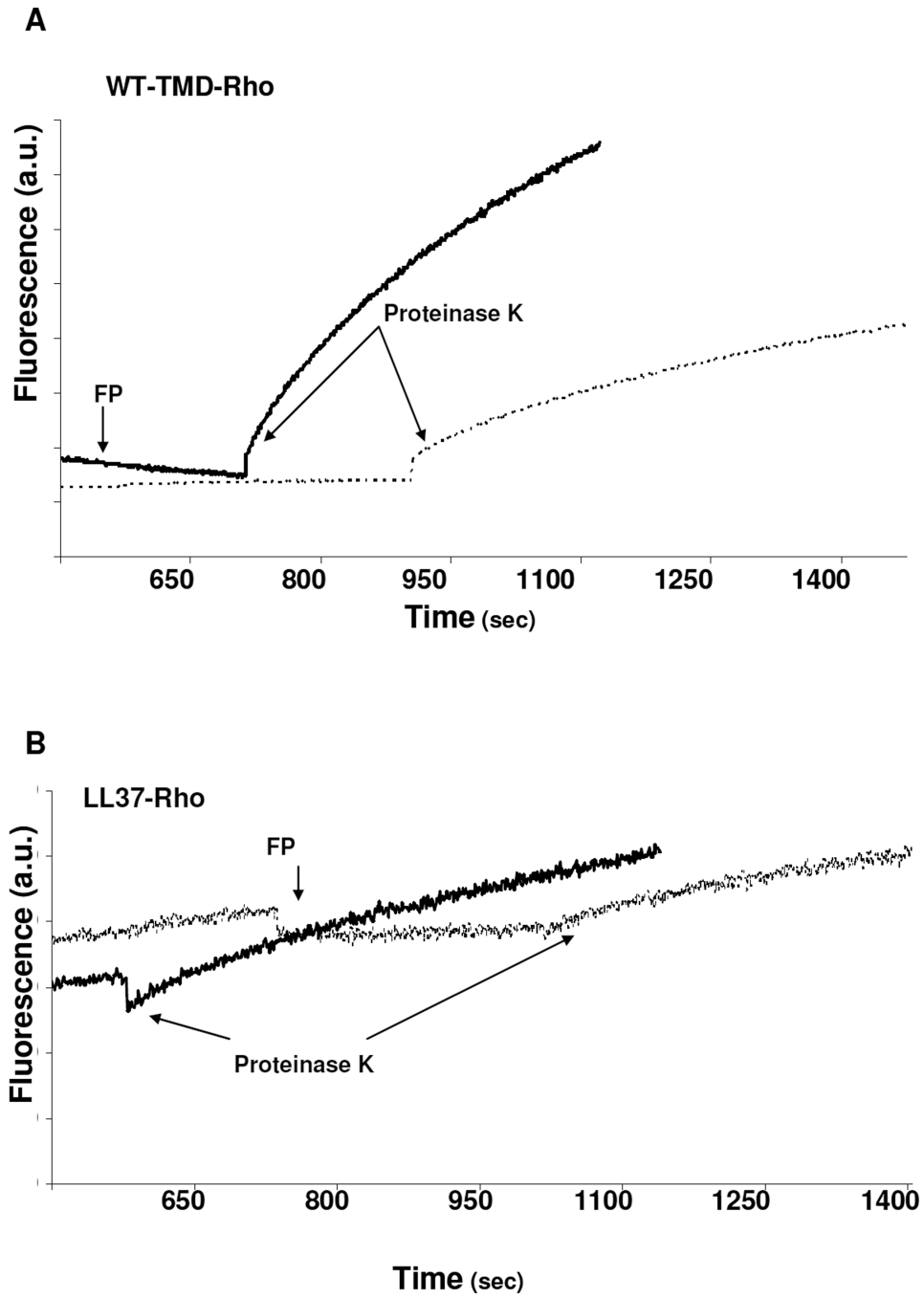

Figure 4. The association of WT-TMD with FP (1–33) leads to a shift in its localization/ organization on model membranes

Rho-labeled WT-TMD (A) peptide and LL37 (B) were added to a solution of 100μM LUVs and allowed to assemble. The emission observed decreased with time as a result of quenching. After the signal stabilized, proteinase K was added (2.4μg), without or after the addition of FP 1–33 (full and dashed lines, respectively). The signal increase upon treatment with the proteinase originates from the dissociation of oligomerized Rho-TMD after enzymatic degradation. In the absence of FP in the system, a rapid cleavage was detected compared to the rate of degradation in the presence of FP. As a control, no difference in the rate of degradation of Rho-LL-37 was observed with or without the presence of FP.

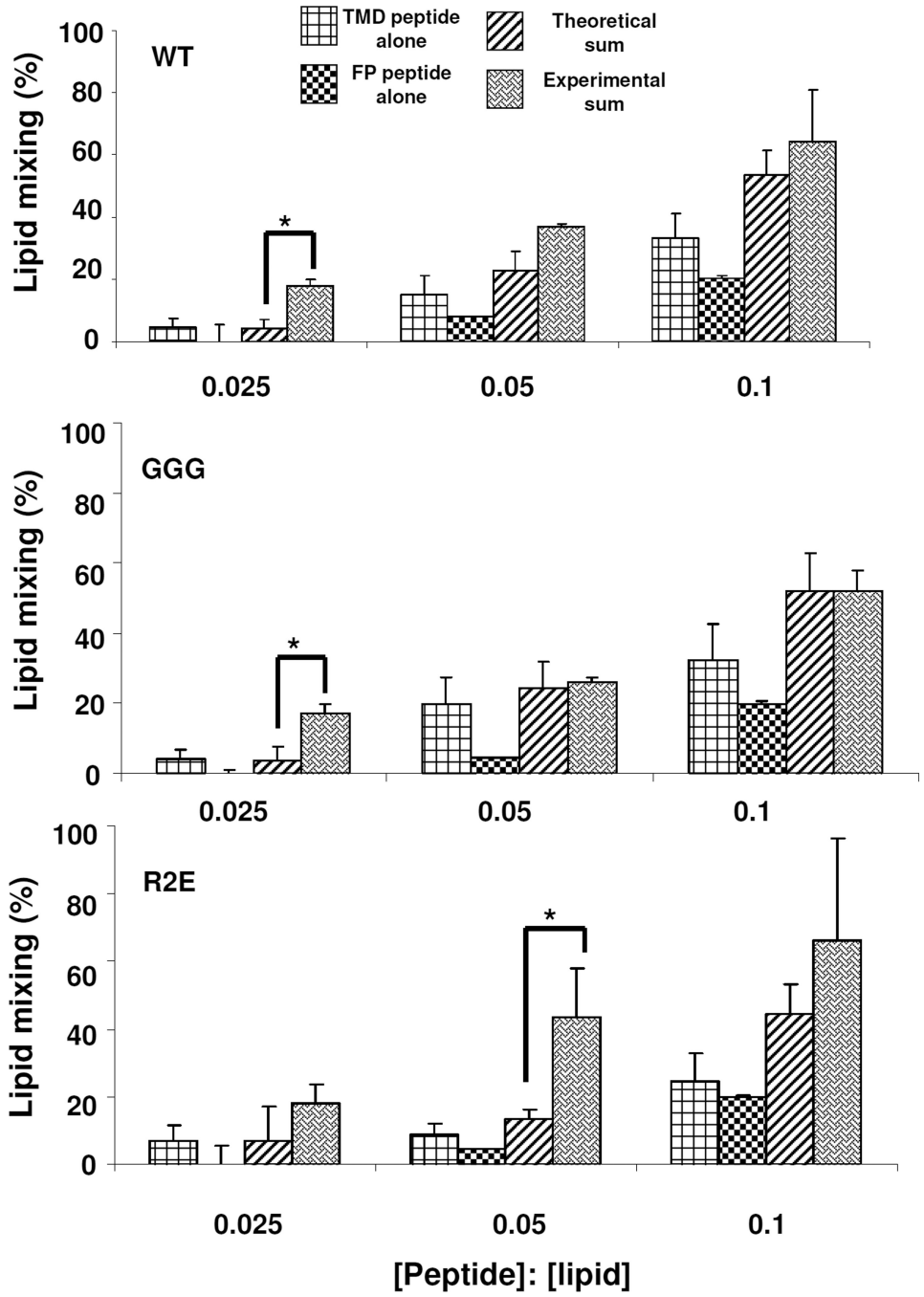

Figure 5. The gp41 TMD and FP cooperate in lipid mixing

Dose-dependent lipid mixing of PC:Chol (9:1) LUV induced by the various TMD peptides alone and together with gp41 FP. Proteins aliquots were added to 100μM LUV containing 10% pre-labeled LUV with 0.6 mol % NBD-PC and Rho-PC in PBS buffer. Increase of NBD fluorescence intensity was measured up to 5 minutes after addition of the peptides. The reference (100% lipid mixing) was the fluorescent signal obtained after the addition of 0.5% Triton to the LUV solution. The percentage of lipid mixing for each TMD alone was plotted for three peptide:lipid molar ratios (0.025, 0.05, and 0.1) and are shown in the corresponding panels. Then FP was examined for its cooperative function together with the three TMD peptides. For each TMD peptide, starting from left to right is the activity of each

TMD peptide alone, FP alone, a theoretical sum of both, and the experimental result of the combination (see designations embedded within Figure 5). As a negative control we measured the signal change induced by addition of DMSO alone and TAR1 TMD peptide; both had no effect on the fluorescent signal. Statistical significance was calculated by student T test (n=3, *- $p<0.05$).

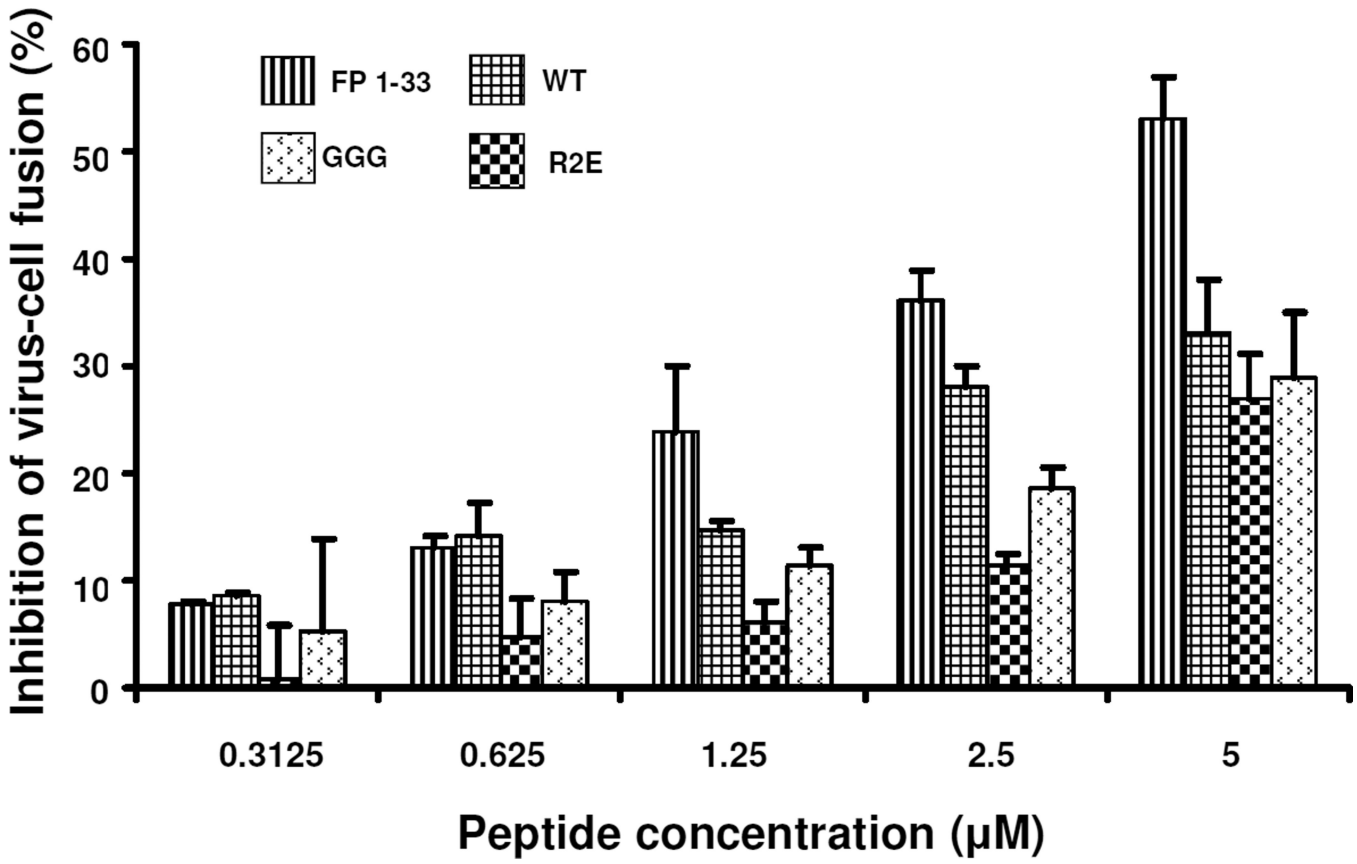

Figure 6. The TMD peptides inhibit virus-cell fusion in a dose-dependent manner

The various TMD peptides or FP (1–33) were added to a mixture of CD4 T cells and HIV viral particles. Designations are embedded within the Figure. Fusion was measured by the expression of Luciferase in the infected cells. Fusion inhibition was calculated as the percentage of Luc expressing cells compared to 1% DMSO-treated cells. The results are the mean of three independent experiments.

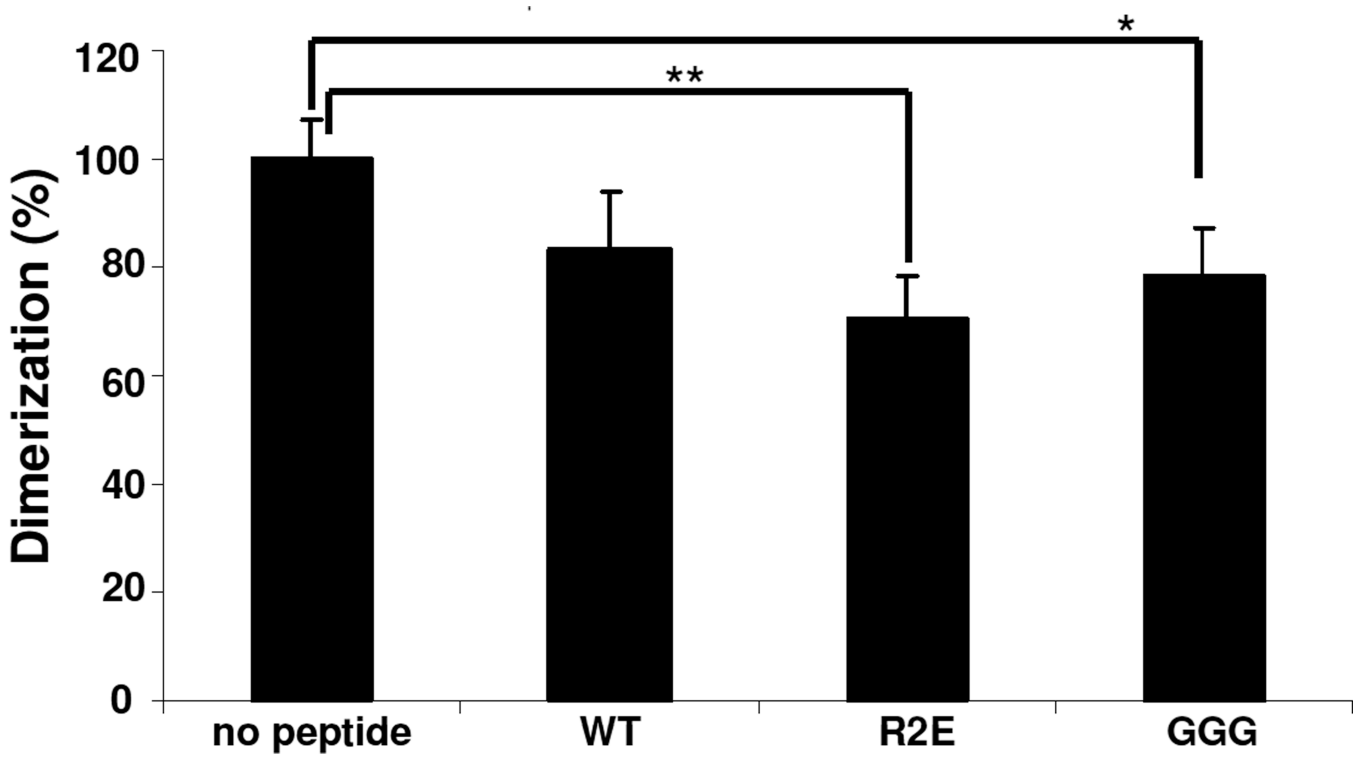

Figure 7. The TMD peptides hetero-associate with gp41 TMD in cell membranes

Cells expressing the ToxR-TM-MalE (WT) chimera were grown in the absence and presence of the TMD peptides, and the extent of lacZ activity was measured. The association of the exogenous peptide with the TM of the chimera causes a decrease in lacZ activity as described in the legend to Figure 3. Statistical significance was calculated by student T-test (n=3, p values= *<0.01).

Table 1

The list of peptides and TM sequences utilized in this study

Construct/peptide name	Sequence	Property
WT	^{686}I V G G L V G L R I V F A V L S^{701}	Wild-type sequence
GGG	I V **G G G L V** L R I V F A V L S	GxxxG Motif abolished
R2E	I V G G L V G L **E** I V F A V L S	Charge exchange
FP	AVGIGALFLGFLGAAGSTMGARSAMTLTVQRQL	Wild-type sequence
Tar1	K K K M V L G V F A L L S L I S G S L K K	Aspartate receptor TMD1
GpA	I T L I I F G V M A G V I G T I L	Partial TMD of GpA

[a] Amino acids are numbered according to their position in the WT protein (HXB2). Mutations in the gp41 TM domain are bold and underlined.

[b] A single Lys residue was added to the N terminus of all the peptides to enhance solubility.